

Effects of hole doping and electron-phonon interaction on the electronic structure of $\text{Ba}_{1-x}\text{K}_x\text{BiO}_3$ studied by photoemission spectroscopy

H. Namatame,* A. Fujimori, and H. Torii

Department of Physics, University of Tokyo, Bunkyo-ku, Tokyo 113, Japan

T. Uchida,† Y. Nagata, and J. Akimitsu

College of Science and Engineering, Aoyama-Gakuin University, Chitosedai Setagaya-ku, Tokyo 157, Japan

(Received 16 May 1994)

The electronic structure of $\text{Ba}_{1-x}\text{K}_x\text{BiO}_3$ has been studied by photoemission spectroscopy. With increasing x , the spectra are generally shifted towards the Fermi level (E_F), indicating a downward shift of E_F due to hole doping. The magnitudes of the shifts, however, are substantially smaller than those predicted by band-structure calculations. In the cubic metallic phase, although band-structure calculations on the cubic structure predict the density of states (DOS) to show a peak at or close to E_F , the photoemission intensity decreases towards E_F , suggesting that the splitting of the Bi 6s band persists and results in a pseudogap behavior. We propose that the suppression of the DOS peak at E_F is caused by dynamical lattice distortion: The DOS peak predicted for the cubic structure presumably induces the lattice instability, leading to the dynamical lattice distortion.

I. INTRODUCTION

The discovery of superconductivity at $T_c \sim 30$ K in $\text{Ba}_{1-x}\text{K}_x\text{BiO}_3$ (BKBO) (Ref. 1) has stimulated reconsideration of superconductivity mechanisms in the closely related system $\text{BaPb}_{1-x}\text{Bi}_x\text{O}_3$ (BPBO; $T_c \sim 13$ K) as well as in the cuprate superconductors. The Bi- and Cu-oxide superconductors have some common characteristic features: (i) The density of states (DOS) at the Fermi level (E_F) is low compared to, e.g., A15 superconductors;² (ii) band-structure calculations³ predict that the E_F is located within a wide, nondegenerate σ -antibonding band; (iii) superconductivity is realized by doping carriers into parent insulators, where the half-filled conduction band is split and opens a band gap. On the other hand, they differ from each other in that the parent compound of the Bi-oxide superconductors is a “charge-density-wave” (CDW) insulator while those of the cuprate superconductors are antiferromagnetic insulators. Also, the crystal structures of the Bi oxides are three dimensional while those of the cuprates are two dimensional. To understand the similarities and differences between the Bi and Cu oxides and their relevance to superconductivity, their electronic structures near E_F and their evolution from the insulators to the superconductors with carrier doping have to be elucidated.

The splitting of the half-filled Bi 6s band in the parent insulator BaBiO_3 is caused by the breathing- and tilting-type lattice distortions of the BiO_6 octahedra.⁴ BKBO becomes metallic and superconducting for K-substitution $x > \sim 0.3$ while BPBO becomes metallic for a larger amount of Pb-substitution $1-x > \sim 0.65$. In previous photoemission and x-ray-absorption (XAS) studies of BPBO, it has been found that Pb substitution induces new (Pb 6s-like) states well above E_F , outside the band gap of the parent compound BaBiO_3 .⁵ This is contrasted with the case of the cuprates, where doping-induced

states (or doping-induced spectral weight) appear near E_F within the band gaps of the parent compounds.⁶ The optical properties of BPBO in the metallic phase shows the coexistence of Drude-type absorption due to free carriers and interband absorption reminiscent of the transitions between the split Bi 6s bands of BaBiO_3 .⁷ This implies a pseudogap behavior in the electronic DOS near E_F , reminiscent of the “CDW” gap of BaBiO_3 , due to dynamical or local lattice distortion in the Pb-substituted compounds.⁸ The photoemission spectra of BPBO (Ref. 5) have indeed shown a decrease of the intensity towards E_F , in contrast to the DOS given by band-structure calculations on the undistorted, cubic lattice,³ which show a pronounced peak at or close to E_F . The optical properties of BKBO in the metallic phase, on the other hand, have been controversial as to whether the interband absorption coexists with the Drude-type absorption or not.^{9–11}

In this work, we have performed a photoemission study of BKBO single crystals with varying K concentration. Resulting spectra, especially of the metallic phase, are found to be similar to those of BPBO except for the overall intensity of the Bi 6s band. That is, we find the emission intensity to decrease towards E_F as in the case of BPBO, indicating a pseudogap behavior similar to that in BPBO. The result is discussed in terms of possible dynamical lattice distortion and strong electron-phonon interaction for the superconducting compositions. So far, several photoemission studies have been reported for BKBO (Ref. 12) but no systematic composition dependence has been studied.

II. EXPERIMENT

Single crystals of $\text{Ba}_{1-x}\text{K}_x\text{BiO}_3$ with $x = 0.3$ ($T_c = 29$ K), 0.38 ($T_c = 30.5$ K), and 0.48 ($T_c = 27$ K) were prepared by an electrochemical method. Since they all

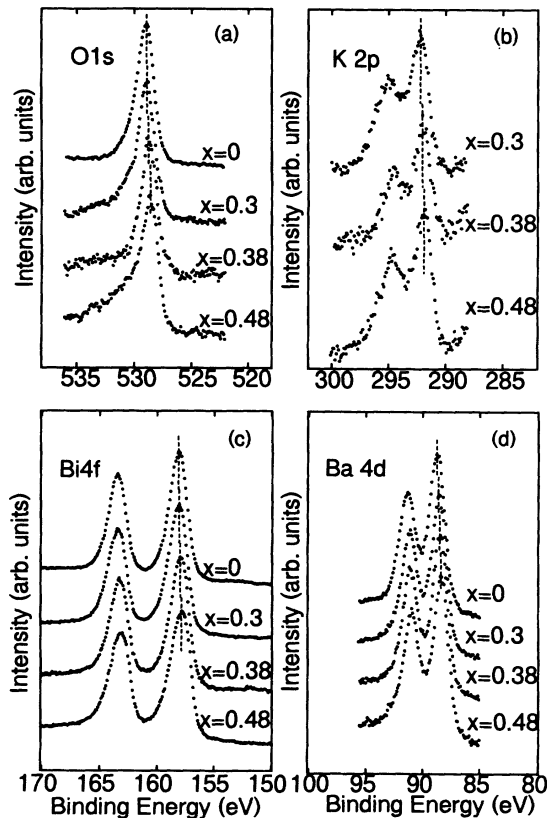


FIG. 1. XPS spectra of the O 1s, Bi 4f, K 2p, and Ba 4d core levels in $\text{Ba}_{1-x}\text{K}_x\text{BiO}_3$.

show metallic conductivity, the metal-semiconductor transition in our samples occurs at $x < 0.3$. The K contents of the samples were determined by a Rietveld analysis of x-ray-diffraction data¹³ and electron-probe microanalysis (EPMA), the results of which agreed with each other. Details of the preparation and characterization of the samples are described in Ref. 14.

Photoemission measurements were performed using a spectrometer equipped with a double-pass cylindrical-mirror analyzer and a He discharge lamp for ultraviolet photoemission spectroscopy (UPS) and a Mg $K\alpha$ x-ray source for x-ray-photoemission spectroscopy (XPS). The total-energy resolution was ~ 0.3 eV for UPS and ~ 0.8 eV for XPS. The base pressure of the spectrometer was $\sim 1 \times 10^{-10}$ Torr. The samples were cooled to liquid-nitrogen temperature in order to minimize possible surface degradation in the ultrahigh vacuum. Clean surfaces were prepared by scraping the samples *in situ* with a diamond file, as described in Ref. 5. The cleanliness of the sample surfaces was checked by the absence of a second feature on the high binding-energy side of the O 1s XPS peak, as shown in Fig. 1(a). The Fermi level of each sample was determined by the Fermi edge of Au evaporated on the sample.

III. RESULTS

XPS spectra of the O 1s, Bi 4f, Ba 4d, and K 2p core levels are shown in Fig. 1. The relative binding energies

of the core levels are plotted in Fig. 2 as functions of x . In going from $x=0$ to 0.48, all the core-level peaks are shifted towards lower binding energies. Therefore the shifts can be interpreted largely as due to an upward shift of E_F caused by the hole doping.

Figure 3 shows the valence-band UPS spectra of BKBO. The spectra of $\text{BaPb}_{0.75}\text{Bi}_{0.25}\text{O}_3$ and BaPbO_3 (Ref. 5) are also shown for comparison. The prominent peak at ~ 3.5 eV is due to (nonbonding) O 2p states; O-2p-Bi-6s bonding states are located around 6–9 eV and O-2p-Bi-6s antibonding states, which are mainly composed of Bi 6s states (referred to as Bi 6s states hereafter), are located near E_F . For BaBiO_3 , the top of the occupied Bi 6s band is located ~ 0.3 eV below E_F . In going from $x=0$ to 0.3, the top of the occupied Bi 6s band moves towards E_F and touches it, indicating that the system becomes barely metallic. At $x=0.38$, for which the highest T_c was observed, the Fermi edge shows the highest intensity. The intensity at E_F is reduced for $x=0.48$, where the solubility limit of K is approached. Note that the intensity at E_F of the “optimally doped” $\text{Ba}_{0.62}\text{K}_{0.38}\text{BiO}_3$ is higher than that of the optimally doped $\text{BaPb}_{0.75}\text{Bi}_{0.25}\text{O}_3$ by a factor of $\lesssim 2$.

In addition to the shift of the top of the Bi 6s band, the peak of the O 2p band is also shifted towards lower binding energies with K substitution (except for $x=0.48$) as shown in Figs. 2 and 3. The shifts of all the spectral features mentioned above suggest that a downward shift of E_F occurs with hole doping, which is caused by the K substitution (although the energy shift as a function of x is not necessarily parallel between the different levels). However, the amount of the shift is smaller than that predicted by the band-structure calculations.³ That is, in go-

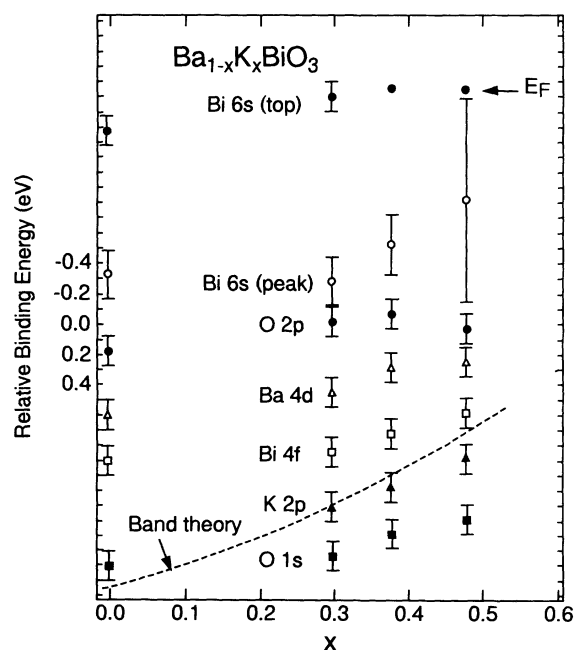


FIG. 2. Binding energies of the core-level and valence-band (O 2p and Bi 6s) peaks as functions of x . The dashed line shows a shift predicted by the band-structure calculations (Ref. 3).

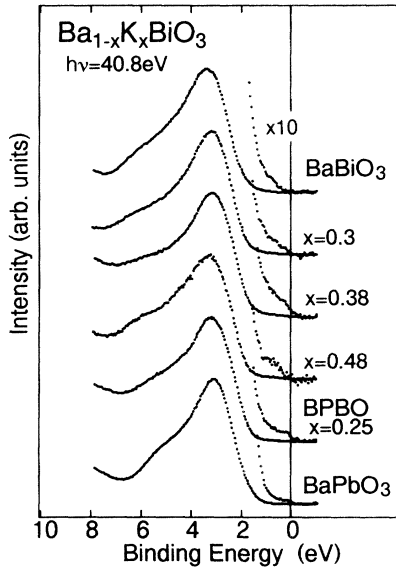


FIG. 3. Valence-band UPS spectra of $\text{Ba}_{1-x}\text{K}_x\text{BiO}_3$ compared with those of $\text{BaPb}_{0.75}\text{Bi}_{0.25}\text{O}_3$ and BaPbO_3 (Ref. 5). A magnified view around E_F is given for each spectrum.

ing from $x=0$ to $x\sim 0.4$, the experimental data show an overall shift of ~ 0.3 eV whereas the band-structure calculations have predicted a shift of ~ 0.9 eV, as shown by a dashed line in Fig. 2.

In order to highlight the contribution of the Bi 6s states to the photoemission spectra, we have subtracted the spectrum of BaPbO_3 from those of BKBO, as shown in Fig. 4. Here we have assumed that the valence band of BaPbO_3 largely consists of O 2p states because the Pb 6s states are located well (~ 2 eV) above E_F .^{5,15} Indeed, the photoemission spectrum of BaPbO_3 within ~ 1 eV of E_F

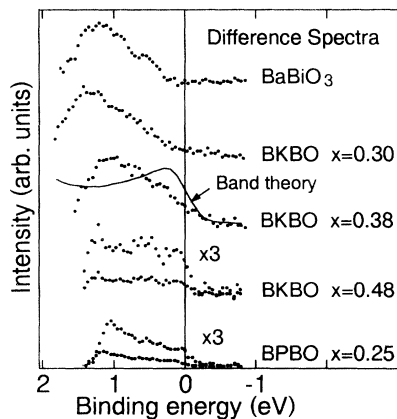


FIG. 4. Difference UPS spectra (dots) between $\text{Ba}_{1-x}\text{K}_x\text{BiO}_3$ and BaPbO_3 and that between $\text{BaPb}_{0.75}\text{Bi}_{0.25}\text{O}_3$ and BaPbO_3 . Prior to subtraction, the spectra have been normalized as described in the text. The solid curve shows the Bi 6s partial DOS given by the band-structure calculation by Mattheiss and Hamann (Ref. 3), broadened with the instrumental resolution.

is weak and shows no appreciable structure. We have also assumed that the O 2p band is not significantly deformed by the K substitution since K-derived states are located well above E_F and work merely as a carrier source. To make the subtraction, the O 2p peak of BaPbO_3 was aligned to those of BKBO and their peak intensities were normalized. The resulting difference spectra are thus attributed to the occupied part of the Bi 6s band. It should be noted that at $x=0.38$, the peak of the Bi 6s band persists while the Fermi edge appears: The photoemission intensity decreases towards E_F although the band-structure calculations³ predict a peak at E_F as shown by a solid curve in Fig. 4. This discrepancy implies the formation of a pseudogap at E_F caused by an effect which is not included in the band-structure calculations. At $x=0.48$, the line shape of the Bi 6s band becomes rather flat and its intensity becomes low. This line shape implies that the Bi 6s band approaches a single conduction band as predicted by the band-structure calculations.

The present result indicates that the integrated intensity of the occupied part of the Bi 6s band is nearly independent of x or decreased only slightly up to $x\sim 0.38$ and then significantly drops at $x=0.48$. In a recent optical study,¹⁰ the x dependence of the carrier density shows a peak around $x=0.35$ corresponding to the maximum in T_c . In an O 1s XAS study,¹⁶ the intensity at the absorption edge increases in going from $x=0$ to 0.2 and then decreases to $x=0.4$. It should be noted in Fig. 4 that the Bi 6s band for the optimally doped BKBO ($x\sim 0.38$) shows a line shape similar to that of the optimally doped BPBO ($x\sim 0.25$) with an overall intensity higher than that of BPBO.

IV. DISCUSSION

The O 1s XAS result on BPBO has shown that Pb substitution creates new states of Pb 6s character *outside* the band gap of BaBiO_3 .⁵ On the other hand, the O 1s XAS data on BKBO (Ref. 16) show an increase in the absorption edge intensity with increasing x , indicating that doping-induced states appear just above E_F , probably *inside* the band gap of BaBiO_3 . In spite of these different behaviors between the Pb- and K-substituted systems, the photoemission spectra show similar behaviors with respect to the line shape and the E_F shift. Note, however, that changes corresponding to those of BKBO from $x=0$ to $x\sim 0.5$ occur in BPBO from $x=1$ to $x\sim 0$. The difference between BPBO and BKBO in the Bi 6s band photoemission intensity and hence in the DOS at E_F may be responsible for the different T_c 's between the two systems.

Let us now discuss the origin of the pseudogap behavior in the photoemission spectra of the metallic phase. The semiconducting behavior of BaBiO_3 has been explained as due to the splitting of the Bi 6s band resulting from the breathing- and tilting-type lattice distortions of the BiO_6 octahedra.⁴ In both BPBO and BKBO, the lattice distortion disappears in the metallic phase and the crystal becomes cubic or nearly cubic.^{13,17} Nevertheless,

extended x-ray-absorption fine-structure (EXAFS) studies of BPBO have identified two Bi-O bond lengths in the superconducting phase, indicating that dynamical or local breathing-type distortion persists in that phase.⁸ If the lattice distortion were completely lost in the metallic phase, the Bi 6s band would become a single band as predicted by the band-structure calculations on the cubic structure and the E_F would lie at or close to the DOS peak of the Bi 6s band. On the contrary, the measured spectra show a peak around 1–1.5 eV below E_F and the intensity decreases towards E_F . While an EXAFS study has found a single Bi-O bond length in superconducting BKBO samples,¹⁶ a recent pair-distribution-function analysis of neutron-diffraction data has indicated that dynamical lattice distortion persists in cubic $\text{Ba}_{0.6}\text{K}_{0.4}\text{BiO}_3$.²⁰ Presumably, the presence of the DOS peak predicted for the average cubic structure causes lattice instability and hence the dynamical distortion, which splits the DOS peak thereby lowering the energy of the electron system. Recently, it has been found that the DOS peak at E_F is suppressed in the photoemission spectra of the new superconductor $\text{YNi}_2\text{B}_2\text{C}$, too.¹⁸ Theoretically, the formation of a pseudogap at E_F due to electron-phonon interaction has been predicted for the Holstein model.¹⁹

The band-structure calculations on BKBO with the cubic structure yield the DOS at E_F to be $N_{\text{band}}(0) \sim 0.23$ states/spin eV cell for $x \sim 0.4$.³ From the photoemission intensity at E_F , the bare (i.e., unenhanced) DOS of the dynamically distorted lattice is evaluated to be $N_{\text{PES}}(0) \sim 0.16$ states/spin eV cell for $x = 0.38$, under the assumption that the integrated Bi 6s spectral weight in the difference spectrum is $\sim 1-x$ states/eV cell. (Note that the photoemission intensity at E_F is not effected by the mass enhancement mentioned below.) The fact that $N_{\text{PES}}(0)$ is suppressed compared to $N_{\text{band}}(0)$ is attributed to the pseudogap formation due to the dynamical lattice distortion [see Fig. 5(c)]. Electrons near E_F in such a dynamically distorted lattice would be dressed by “phonon clouds” and therefore the quasiparticle DOS at E_F $N^*(0)$ would be enhanced. Indeed, electronic specific-heat measurements of $\text{Ba}_{0.6}\text{K}_{0.4}\text{BiO}_3$ have yielded $N^*(0) \sim 0.32$ states/spin eV cell,²¹ giving a mass enhancement factor $N^*(0)/N_{\text{band}}(0) \sim 1.4$. Qualitatively the same relationship between $N_{\text{band}}(0)$, $N^*(0)$ and $N_{\text{PES}}(0)$, i.e., the suppression of $N_{\text{PES}}(0)$ and the enhancement of $N^*(0)$ compared to $N_{\text{band}}(0)$, has been found for BPBO:⁵ $N_{\text{band}}(0) \sim 0.13$ states/spin eV cell, $N_{\text{PES}}(0) \sim 0.10$ states/spin eV cell and $N^*(0) \sim 0.14$ states/spin eV cell.²²

The pseudogap behavior in the optical spectra, namely, the coexistence of the Drude absorption and the interband transition, has been well established for BPBO; the interband transition occurs between the split Bi 6s bands.⁷ On the other hand, optical studies of BKBO by Sato *et al.*¹¹ did not show such a pseudogap in the metallic region while other optical studies^{9,10} have identified a pseudogap, which tends to collapse with increasing x but persists into the metallic region. Presumably in BKBO, considerable amount of spectral weight is transferred

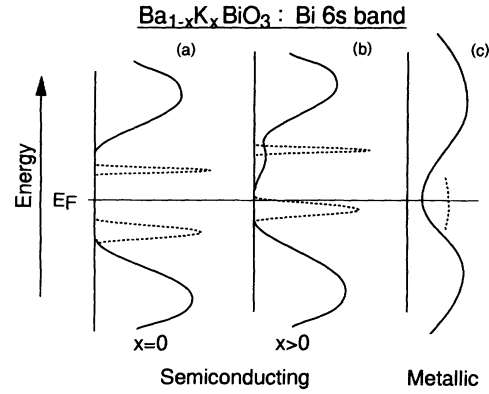


FIG. 5. Schematic electronic structure of $\text{Ba}_{1-x}\text{K}_x\text{BiO}_3$ near the Fermi level. The solid curves represent the photoemission spectra or the spectral density $N_{\text{PES}}(\epsilon)$, which can be reached by the sudden removal or addition of an electron, and the dashed curves represent the quasiparticle density of states $N^*(\epsilon)$, which governs the thermal and transport properties.

from the interband absorption region to the Drude absorption, because of the larger number of free carriers as reflected on the higher DOS at E_F , thereby obscuring the interband feature.

Finally, the small shift of E_F (~ 0.3 eV) with hole doping compared to that predicted by the band-structure calculations (~ 0.9 eV) may be understood as a result of strong electron-phonon interaction as follows. It has been shown from an analysis of the photoemission spectra that electron-phonon interaction leads to the formation of a narrow polaronic band within the band gap of BaBiO_3 as indicated by dashed lines in Fig. 5(a).⁵ The polaronic hole band is located slightly (~ 0.25 eV) below E_F and accommodates doped hole carriers. Upon hole doping, therefore, the E_F is shifted to the top of the polaronic hole band as shown in Fig. 5(b). (The figure also shows that extra spectral weight which appears above E_F , probably within the band gap of BaBiO_3 .) As the hole doping further proceeds, the band gap collapses and the ordinary band model partially recovers even though a pseudogap survives [Fig. 5(c)], resulting in the partial recovery of the E_F shift as a function of x . Indeed, Fig. 2 indicates that the core-level shifts in the metallic region ($x > \sim 0.3$) amount to approximately half of those predicted by the band-structure calculations.

V. CONCLUSIONS

We have investigated the electronic structure of BKBO for a wide composition range using photoemission spectroscopy. With K substitution, the occupied part of the split Bi 6s band, which shows a peak ~ 1 eV below E_F , is shifted towards E_F and a Fermi edge appears in the metallic phase. The photoemission spectra show a pseudogap behavior in the metallic phase as in the case of BPBO and the pseudogap tends to vanish towards the solubility limit of K, $x \sim 0.5$. The changes of the Bi 6s states in BKBO and BPBO as a function of chemical composition

thus resemble each other, although on the different x scales, except for the overall photoemission intensity. In particular, the line shape of the Bi 6s band for the optimally doped BKBO ($x \sim 0.38$) is similar to that of the optimally doped BPBO ($x \sim 0.25$) with an overall intensity higher than that of BPBO. The different DOS at E_F may be responsible for the different T_c 's between the two systems. We propose that dynamical structural distortion existing in the metallic phase suppresses the DOS peak at E_F , which has been predicted for the average cubic structure, and leads to the pseudogap behavior. At the same time, electron-phonon interaction enhances the quasiparticle DOS at E_F as reflected on the electronic specific heat. The dynamical instability of the cubic lattice is probably caused by the presence of the DOS peak at E_F predicted for the cubic structure.

Considering the fact that evidence for dynamical lattice distortion has been found in many cuprate supercon-

ductors,²³ their electronic structures would have to be reexamined under the influence of such a lattice distortion and strong electron-phonon interaction. Indeed, the small E_F shift between n -type and p -type cuprates observed by photoemission spectroscopy²⁴ has not been explained so far within models of correlated electrons and therefore one may have to take into account the effects of electron-phonon interaction to explain the experimental results.

ACKNOWLEDGMENTS

The BaBiO₃ sample was supplied by H. Takagi. We acknowledge the support of a Grant-in-Aide for Scientific Research from the Ministry of Education, Science, and Culture, Japan. The work at Aoyama-Gakuin University was supported by a grant from the Research Institute of Aoyama-Gakuin University.

*Present address: Department of Materials Science, Hiroshima University, Higashi-Hiroshima 724, Japan.

†Present address: Department of Image Information Engineering, Tokyo Institute of Polytechnics, Atsugi 243, Japan.

¹L. F. Mattheiss, E. M. Gyorgy, and D. W. Johnston, Jr., *Phys. Rev. B* **37**, 3745 (1988); R. J. Cava, B. Batlogg, J. J. Krajewski, R. Farrow, L. W. Rupp, Jr., A. E. White, K. Short, W. F. Peck, and T. Kometani, *Nature* **332**, 814 (1988).

²B. Batlogg, *Physica C* **185-189**, xviii (1991).

³BPBO: L. F. Mattheiss and D. R. Hamann, *Phys. Rev. B* **28**, 4227 (1983); K. Takegahara and T. Kasuya, *J. Phys. Soc. Jpn.* **56**, 1478 (1987). BKBO: L. F. Mattheiss and D. R. Hamann, *Phys. Rev. Lett.* **60**, 2681 (1988); N. Hamada, S. Massidda, A. J. Freeman, and J. Redinger, *Phys. Rev. B* **40**, 4442 (1989).

⁴A. I. Liechtenstein, I. I. Mazin, C. O. Rodriguez, O. Jepsen, O. K. Anderson, and M. Methfessel, *Phys. Rev. B* **44**, 5388 (1991).

⁵H. Namatame, A. Fujimori, H. Takagi, S. Uchida, F. M. F. de Groot, and J. C. Fuggle, *Phys. Rev. B* **48**, 16917 (1993).

⁶See, e.g., A. Fujimori and H. Namatame, *Physica C* **185-189**, 51 (1991).

⁷S. Tajima, S. Uchida, A. Masaki, H. Takagi, K. Kitazawa, S. Tanaka, and A. Katsui, *Phys. Rev. B* **32**, 6302 (1985); S. Tajima, S. Uchida, A. Masaki, H. Takagi, K. Kitazawa, S. Tanaka, and S. Sugai, *ibid.* **35**, 696 (1987).

⁸J. B. Boyce, F. G. Bridges, T. Claeson, T. H. Geballe, G. G. Li, and A. W. Sleight, *Phys. Rev. B* **44**, 6961 (1991).

⁹Z. Schlesinger, R. T. Collins, J. A. Calise, D. G. Hinks, A. W. Mitchell, Y. Zheng, B. Dabrowski, N. E. Bickers, and D. J. Scalapino, *Phys. Rev. B* **40**, 6862 (1989); S. H. Blanton, R. T. Collins, K. H. Kelleher, L. D. Rotter, Z. Schlesinger, D. G. Hinks, and Y. Zheng, *ibid.* **47**, 996 (1993).

¹⁰M. A. Karlow, S. L. Cooper, A. L. Kotz, M. V. Klein, P. D. Han, and D. A. Payne, *Phys. Rev. B* **48**, 6499 (1993).

¹¹H. Sato, S. Tajima, H. Takagi, and S. Uchida, *Nature* **338**, 241 (1989); H. Sato, T. Ido, S. Uchida, S. Tajima, K. Yoshida, K. Tanabe, K. Tatsuhara, and N. Miura, *Phys. Rev. B* **48**, 6626 (1993); S. Tajima, M. Yoshida, N. Koshizuka, H. Sato, and S. Uchida, *ibid.* **46**, 1232 (1992).

¹²For example, T. J. Wagener, H. M. Meyer III, D. M. Hill, Y.-

J. Hu, N. B. Jost, J. H. Weaver, D. G. Hinks, B. Dabrowski, and D. R. Richards, *Phys. Rev. B* **40**, 4532 (1989); Y. Joen, G. Liang, J. Chen, M. Croft, M. W. Ruckman, D. Di Marzio, and M. S. Hegde, *ibid.* **41**, 4066 (1990).

¹³S. Pei, J. D. Jorgensen, B. Dabrowski, D. G. Hinks, D. R. Richards, A. W. Mitchell, J. M. Newsam, S. K. Shinha, D. Vaknin, and A. J. Jacobson, *Phys. Rev. B* **41**, 4126 (1990).

¹⁴Y. Nagata, N. Suzuki, T. Uchida, W. D. Mosley, P. Klavins, and R. N. Shelton, *Physica C* **195**, 195 (1992); T. Uchida, S. Nakamura, N. Suzuki, Y. Nagata, W. D. Mosley, M. D. Lan, P. Klavins, and R. N. Shelton, *ibid.* **215**, 350 (1993).

¹⁵F. M. F. de Groot, J. C. Fuggle, and J. M. van Ruitenbeek, *Phys. Rev. B* **44**, 5280 (1991).

¹⁶S. Salem-Sugui, Jr., E. E. Alp, S. M. Mini, M. Ramanathan, J. C. Campuzano, G. Jennings, M. Faiz, S. Pei, B. Dabrowski, Y. Zheng, D. R. Richards, and D. G. Hinks, *Phys. Rev. B* **43**, 5511 (1991).

¹⁷D. T. Marx, P. G. Radaelli, J. D. Jorgensen, R. L. Hitterman, D. G. Hinks, S. Pei, and B. Dabrowski, *Phys. Rev. B* **46**, 1144 (1992).

¹⁸A. Fujimori, K. Kobayashi, T. Mizokawa, K. Mamiya, A. Sekiyama, H. Eisaki, H. Takagi, S. Uchida, R. J. Cava, J. J. Krajewski, and W. F. Peck, Jr., *Phys. Rev. B* (to be published).

¹⁹M. Vekic and S. R. White, *Phys. Rev. B* **48**, 7043 (1993).

²⁰H. D. Rosenfeld and T. Egami, in *Lattice Effects in High- T_c Superconductors*, edited by Y. Bar-Yam and T. Egami (World Scientific, Singapore, 1992), p. 105.

²¹J. E. Graebner, L. F. Schneemeyer, and J. K. Thomas, *Phys. Rev. B* **39**, 9682 (1989).

²²In Ref. 5, the unit "states/eV cell" should be replaced by "states/spin eV cell."

²³B. H. Toby, T. Egami, J. D. Jorgensen, and M. A. Subramanian, *Phys. Rev. Lett.* **64**, 2414 (1990).

²⁴H. Namatame, A. Fujimori, Y. Tokura, M. Nakamura, K. Yamaguchi, A. Misu, H. Matsubara, S. Suga, H. Eisaki, T. Ito, H. Takagi, and S. Uchida, *Phys. Rev. B* **41**, 7205 (1990); J. W. Allen, G. C. Olson, M. B. Maple, J. S. Kang, L. Z. Liu, J. H. Park, R. O. Anderson, W. P. Ellis, J. T. M. Markert, Y. Daliachouch, and R. Liu, *Phys. Rev. Lett.* **64**, 595 (1990).